Cascade biocatalysis systems for bioactive naringenin glucosides and quercetin rhamnoside production from sucrose

Samir Bahadur Thapa[1] · Ramesh Prasad Pandey[1,2] · Puspalata Bashyal[1] · Tokutaro Yamaguchi[2] · Jae Kyung Sohng[1,2]

Abstract

Two sustainable and cost-effective cascade enzymatic systems were developed to regenerate uridine diphosphate (UDP)-α-D-glucose and UDP-β-L-rhamnose from sucrose. The systems were coupled with the UDP generating glycosylation reactions of UDP sugar–dependent glycosyltransferase (UGT) enzymes mediated reactions. As a result, the UDP generated as a by-product of the GT-mediated reactions was recycled. In the first system, YjiC, a UGT from *Bacillus licheniformis* DSM 13, was used for transferring glucose from UDP-α-D-glucose to naringenin, in which AtSUS1 from *Arabidopsis thaliana* was used to synthesize UDP-α-D-glucose and fructose as a by-product from sucrose. In the second system, flavonol 7-*O*-rhamnosyltransferase (AtUGT89C1) from *A. thaliana* was used to transfer rhamnose from UDP-β-L-rhamnose to quercetin, in which AtSUS1 along with UDP-β-L-rhamnose synthase (AtRHM1), also from *A. thaliana*, were used to produce UDP-β-L-rhamnose from the same starter sucrose. The established UDP recycling system for the production of naringenin glucosides was engineered and optimized for several reaction parameters that included temperature, metal ions, NDPs, pH, substrate ratio, and enzymes ratio, to develop a highly feasible system for large-scale production of different derivatives of naringenin and other natural products glucosides, using inexpensive starting materials. The developed system showed the conversion of about 37 mM of naringenin into three different glucosides, namely naringenin, 7-*O*-β-D-glucoside, naringenin, 4′-*O*-β-D-glucoside, and naringenin, 4′,7-*O*-β-D-diglucoside. The UDP recycling (RC_{max}) was 20.10 for naringenin glucosides. Similarly, the conversion of quercetin to quercetin 7-*O*-α-L-rhamnoside reached a RC_{max} value of 10.0.

Keywords Glucosylation · UDP recycling · Sucrose synthase · Rhamnosylation · Cascade biocatalysis

✉ Jae Kyung Sohng
  sohng@sunmoon.ac.kr

[1] Department of Life Science and Biochemical Engineering, Sun Moon University, 70 Sunmoon-ro 221, Tangjeong-myeon, Asan-si, Chungnam 31460, Korea

[2] Department of Pharmaceutical Engineering and Biotechnology, Sun Moon University, 70 Sunmoon-ro 221, Tangjeong-myeon, Asan-si, Chungnam 31460, Korea

Introduction

Naringenin, one of the major citrus flavonoids predominantly found in grapes and oranges (Rouseff et al. 1987), is a naturally occurring optically active compound that is considered to have bioactive effects on human health as an antioxidant, free radical scavenger, anti-inflammatory, carbohydrate metabolism promoter, and as an immunity system modulator (Du et al. 2009; Yıldız et al. 2009; Cavia-Saiz et al. 2010; Leonardi et al. 2010; Qin et al. 2011). Unfortunately, this bioflavonoid is difficult to absorb after oral ingestion. In the best scale scenario, only 15% of ingested naringenin will be absorbed into the human gastrointestinal tract (Felgines et al. 2000; Manach and Donovan 2004).

Glycosylation is one of the very effective and popular methods of modifying natural products, including plant polyphenols such as flavonoids, to increase their pharmacological and pharmacodynamics characters by enhancing their solubility, bioavailability, stability, and bioactivity (Cavia-Saiz et al. 2010; Lewandowska et al. 2013; Khan et al. 2015). Because of the huge biological impact of flavonoids on humans, crude

plant extracts alone might not satisfy the necessary requirements, as they are contained in plants in low amount, and require a long and difficult process of extraction and purification, through an environmentally unfriendly process (Kumar and Pandey 2013; Mei et al. 2015; Panche et al. 2016). There are different methods of glycosylation, such as chemical synthesis, microbial biosynthesis, and enzymatic modifications. Though the chemical synthesis is used for the production of glycosylated flavonoids (Danishefsky and Bilodeau 1996; Nicolaou and Mitchell 2001), it is a complicated process, and suffers from many problems, such as strict reaction conditions, use of protection and deprotection groups, lack of suitable sugar donating groups, less stereospecificity and regioselectivity, and difficulty in purification, resulting in high cost and longer time for production (Xie et al. 2018). To overcome these obstacles, microbial biosynthesis systems are engineered with sugar biosynthetic pathway genes and glycosyltransferases (GTs) from heterologous sources for the production of glycosylated flavonoids (Simkhada et al. 2010; Trantas et al. 2015; Kim et al. 2015; Pandey et al. 2016; Chouhan et al. 2017). However, the process to synthesize diverse sugars conjugated products is limited, due to the lesser conversion of substrate to products, and difficulty of channeling target NDP-sugar pool in the cell cytosol, despite an easy and safe process (Muthana et al. 2012; Pandey et al. 2015). Moreover, some of the metabolites at higher concentration are toxic to the engineered cell (Kim et al. 2014; Shomar et al. 2018). Thus, in vitro enzymatic glycosylation is an alternative approach that is often applied for the production of glycosylated derivatives. But it uses very expensive cofactors and sugar donors for the production of targeted compounds, limiting the scale-up process of the enzymatic synthesis of glycosides at the industrial level (Pandey et al. 2014; Zhang et al. 2014).

Several NDP sugars regenerating cascade reaction systems have been developed by our group and also from other labs Rosencrantz et al. 2014; Gutmann et al. 2014; Le et al. 2014; Gurung et al. 2016; Darsandhari et al. 2018). Though these approaches recycle UDP/TDP efficiently, the system suffers from the production of by-product such as acetate, which while progressing the reaction, decreases the pH of the reaction buffer. Amylosucrase enzymes are also used for the direct transglycosylation of polyphenols, such as resveratrol and other flavonoids (Park et al. 2012; Lee et al. 2018; Tian et al. 2018; Jang et al. 2018). However, the glycodiversification of natural products using amylosucrase is a challenging task, though a few studies have attempted to engineer these enzymes to enhance their tolerance towards diverse sucrose analogs (Daudé et al. 2014; Xu et al. 2016). An alternative approach of utilizing sucrose as the starting material to generate UDP-glucose using sucrose synthase enzyme was also previously utilized for the production of diverse flavonoid glycosides (Masada et al. 2007; De Bruyn et al. 2015; Pei et al. 2017; Gutmann et al. 2017).

In this study, we employ a similar sucrose synthase enzyme to develop diverse NDP-glucoses and NDP-rhamnoses producing systems, using sucrose as the source of glucose and rhamnose moieties (Fig. 1). This study facilitates the possible synthesis of NDP-glucoses and NDP-rhamnoses in one-step and two-step enzymatic reactions, respectively. Both of these systems are coupled with different GT-mediated reactions, thus recycling NDP for a continuous supply of NDP-glucose and NDP-rhamnose for the production of flavonoid glycosides (Fig. 1). The systems are optimized for various parameters for the efficient production of glycosides.

Materials and methods

Chemicals and reagents

Adenosine diphosphate (ADP), thymidine diphosphate (TDP), guanosine diphosphate (GDP), cytosine diphosphate (CDP), uridine diphosphate (UDP), UDP-α-D-glucose (UDP-Glc), thymidine diphosphate-L-rhamnose (TDP-rhamnose), isopropyl-β-D-thiogalactopyranoside (IPTG), and sucrose were purchased from GeneChem Inc. (Daejeon, Korea). Quercetin, NAD$^+$, and NADH were purchased from Sigma-Aldrich (St. Louis, MO, USA), whereas naringenin (purity 98%) was bought from Xi'an Sino-Future Bio-Tech Co., Ltd. (Xi'an, China). Luria-Bertani medium was purchased from KisanBio (Seoul, Korea). All other chemicals and reagents were of the highest chemical grade, and were obtained from different sources. High-performance liquid chromatography (HPLC) grade acetonitrile and water were purchased from Mallinckrodt Baker (Phillipsburg, NJ, USA).

Strains and plasmids

Escherichia coli BL21 (DE3) (Stratagene, La Jolla, CA, USA) was used as a host organism to overexpress recombinant proteins. The pQE30-AtSUS1 plasmid was provided by Professor Hajime Mizukami (Nagoya City University, Japan) (Masada et al. 2007). Previously constructed pET28a-YjiC plasmids (Pandey et al. 2013), pET32b-AtRHM1, and pET41b-AtUGT89C1 (Roepke and Bozzo 2013; Parajuli et al. 2015) were used for the overexpression and production of enzymes. Prior to use, the plasmids were confirmed by restriction enzyme digestion studies.

Culture conditions

E. coli strains were grown in LB broth or an agar plate supplemented when necessary with an appropriate amount of antibiotics (ampicillin, 100 μg/mL; kanamycin, 50 μg/mL). Four recombinant strains *E. coli* BL21 (DE3) harboring pET28a-YjiC, pET32b-AtRHM1, pET41b-AtUGT89C1,

Fig. 1 Cascade reaction schemes. **a** The reaction catalyzed by sucrose synthase to synthesize sucrose from UDP-glucose and fructose. **b** Cascade reaction for the biosynthesis of UDP-glucose from sucrose using AtSUS1 and consecutive glucosyltransferase reaction by YjiC to produce naringenin glucosides. **c** Cascade reaction for the biosynthesis of UDP-rhamnose from sucrose using AtSUS1 and AtRHM1. The rhamnose moiety was successively transferred to quercetin by UGT89C1
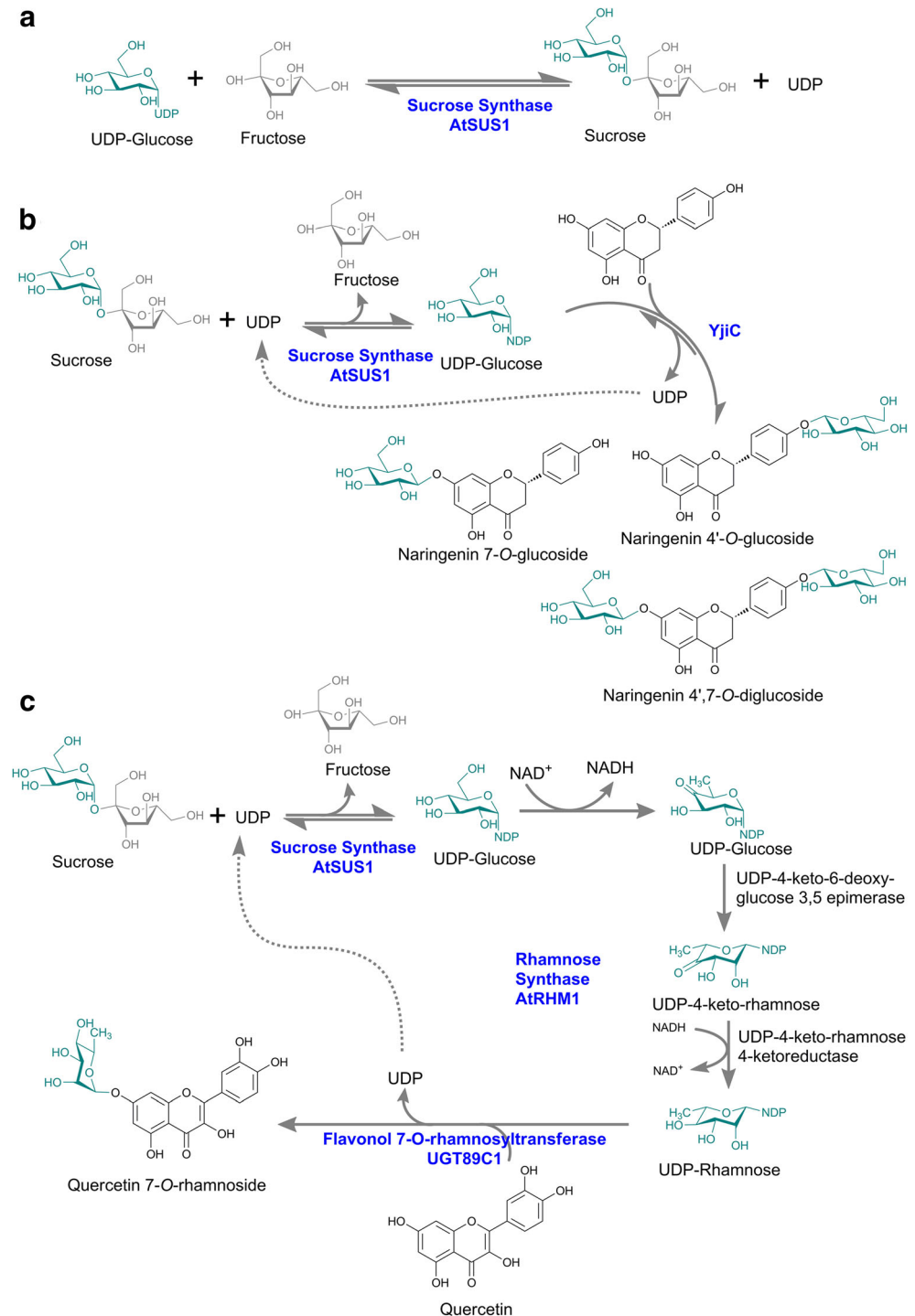
and pQE30-AtSUS1 were prepared by the heat shock transformation method.

Protein expression and analysis

The seed culture of these four strains was prepared in LB broth medium supplemented with corresponding antibiotics, and incubated at 37 °C overnight in a shaking incubator at 200 rpm. Then 500 μL of seed culture was transferred to fresh 100 mL LB medium with the respective antibiotics in 500-mL conical flasks. Once the optical density (OD) at 600 nm reached 0.6, the cultures were induced with 0.4 mM IPTG, and incubated for around 20 h at 20 °C in shaking incubator at 200 rpm. The cell pellets were then harvested by centrifugation at $842 \times g$ (3000 rpm) for 10 min, and washed (vortexed, followed by centrifugation) with buffer (50 mM Tris-HCl and

10% glycerol of pH 7.5) two times, and re-suspended with 1 mL of the same buffer. The cell pellets were lysed using a Fisher Scientific Sonic Dismembrator Model 500 (5–9 s pulse on and off, total 360 s, at 20% amplitude) in an ice bath, and the clear lysate was collected by high-speed centrifugation at 12,000 rpm (13,475×g) for 30 min at 4 °C. The crude protein obtained was further analyzed by 12% sodium dodecyl sulfate-polyacrylamide gel electrophoresis (SDS-PAGE). The protein was stored in a buffer containing 50 mM Tris-HCl, pH 7.5, and 10% glycerol at − 20 °C. The crude protein concentrations were determined by using the Bradford method, with bovine serum albumin as the standard (Bradford 1976).

Regular glucosylation reaction using YjiC

At first, the activity of the YjiC enzyme was checked by conducting the in vitro reaction in 100 mM Tris-HCl (pH 7.5) buffer containing 10 mM MgCl$_2$·6H$_2$O, 3 mM UDP-α-D-glucose, 1 mM naringenin, and YjiC (1.0 μg/mL) in 500 μL volume in a 1.5-mL micro-centrifuge tube. The 10% dimethyl sulfoxide (DMSO) was used as a co-solvent to efficiently dissolve naringenin in the reaction mixture. The reaction assay was incubated at 37 °C for 5 h and the reaction was quenched by adding chilled methanol with vortexing for 10 min. The sample was analyzed by the reverse-phase high-performance liquid chromatography (RP-HPLC)-photo diode array (PDA).

Glucosylation of naringenin (NRN) using sucrose

Two enzymes AtSUS1 (1.0 μg/mL) and YjiC (1.0 μg/mL) were used together to start the reaction from sucrose. The reaction was carried out in 500 μL total volume using 100 mM Tris-HCl (pH 7.5) containing 10 mM MgCl$_2$· 6H$_2$O, 1 mM UDP-α-D-glucose, 300 mM sucrose, and 5 mM naringenin. DMSO at 10% of final reaction volume was used as co-solvent in the reaction mixture. The reaction mixtures were incubated at 37 °C for 20 h. During the reaction, 50 μL samples was collected at 3, 6, 10, and 20 h, and the reaction was quenched by adding 750 μL chilled methanol, and mixed by vortexing for 10 min. Then, the aliquots were centrifuged at 12,000 rpm (13,475×g) to remove denatured proteins. After that, the samples were analyzed by the RP-HPLC. Assay mixtures lacking enzymes and substrate naringenin served as negative and positive controls, respectively.

Cascade reaction optimization

Enzyme concentration variation

Different enzymatic reaction conditions were set up by using YjiC and AtSUS1 enzymes. The one-pot reaction with two enzymes (1:1 ratio of YjiC and AtSUS1 by concentration) was set up by using identical reactions ingredients as the above. Likewise, other reactions were carried out using (1:2, 1:5, 1:10, and 10:1) ratios of YjiC and AtSUS1 enzymes. All the reaction sets were incubated at 37 °C for 20 h. The samples were analyzed by RP-HPLC, after quenching the reaction with chilled methanol.

Variation of UDP-α-D-glucose and naringenin concentration

The experiment conditions were changed by varying UDP-α-D-glucose concentration as follows: 0., 0.2, 0.4, 0.6, 0.8, and 1.0 mM while keeping other components constant, as mentioned above. The concentrations of YjiC and AtSUS1 were maintained in the ratio of 1:10. The naringenin was used at 5 mM concentration. The reactions were analyzed after 20 h incubation. Likewise, other sets of reactions were made by changing the concentrations of naringenin as 5, 8, 10, and 12 mM, while keeping the rest of reaction components unchanged in the reaction assays, to find the effect of changing concentrations of donor and acceptor substrates. UDP-α-D-glucose was used at 1 mM concentration, and the reaction was analyzed by reverse-phase HPLC after 20 h.

Temperature optimization

Similarly, identical sets of the reactions were carried out in 500 μL total volume using 100 mM Tris-HCl (pH 7.5), 10 mM MgCl$_2$·6H$_2$O, 1 mM UDP-α-D-glucose, 300 mM sucrose, 5 mM naringenin, and 10% DMSO to the final concentration of the reaction mixture. During the reactions, the concentrations of YjiC and AtSUS1 were maintained in the ratio of 1:10. Then the reactions assays were incubated at 4, 20, 30, 40, 50, and 60 °C, separately for 20 h. After 20 h, the samples were analyzed.

Buffer optimization

To determine the optimal pH, identical sets of reaction conditions were made as in the temperature optimization reactions, but varying the pH of acetate buffer range of pH (2.93 to 4.19), phosphate buffer of range (6 and 8.1), working Tris-HCl buffer of pH 7.5, and glycine buffer with pH range (9 and 10.2), and the reactions were carried out for 20 h in 37 °C.

Effect of metal ions

The divalent metals Mn^{2+}, Pb^{2+}, Zn^{2+}, Fe^{2+}, Ni^{2+}, Ca^{2+}, Cu^{2+}, Co^{2+}, Mg^{2+}, and Hg^{2+} were used instead of Mg^{2+} solution, separately, and their effect was studied in the formation of glucosylated products with naringenin. The reaction assays were prepared to contain 300 mM sucrose, 1 mM UDP-α-D-glucose, 100 mM Tris-HCl, 5 mM naringenin, and YjiC and

AtSUS1 enzymes in the ratio 1:10 in concentration. The incubation temperature was maintained at 37 °C for 20 h duration.

Reaction assay with NDP

Five different nucleotide diphosphates ADP, CDP, GDP, TDP, and UDP were used separately instead of UDP-α-D-glucose under the same reaction conditions of naringenin glucosylation, using the two enzymes YjiC and AtSUS1 in the ratio 1:10 in concentration. Separate reactions were carried out for each NDP. During the reaction, 300 mM sucrose, 10 mM $MgCl_2 \cdot 6H_2O$, 100 mM Tris-HCl, and 1 mM each NDP were used in 500 μL total reaction volume.

Preparative scale production of naringenin glucosides

The large-scale production reaction was carried out by using 2 mM UDP-α-D-glucose, 10 mM $MgCl_2 \cdot 6H_2O$, 300 mM Tris-HCl, 500 mM sucrose, and 5 mM naringenin and making the concentration of YjiC and AtSUS1 in the ratio 1:10. The 10% DMSO was used as an organic co-solvent to solubilize naringenin in the reaction mixture. The reaction assay was incubated in a shaking incubator at 37 °C. Most importantly, the fed-batch scale-up reaction of naringenin glucosides formation was carried out in a 50-mL tube with a starting volume of reaction mixture 20 mL for 76 h. The samples were analyzed at different time intervals. During the reaction, the concentration ratio of YjiC and AtSUS1 enzymes was maintained at 1:10. The reaction samples were taken at different time points from 10 to 76 h for the analysis of glucoside products in terms of the conversion of naringenin. Though the reaction was started with 5 mM naringenin, an additional 5 mM naringenin was added after 10, 22, 30, 36, 42, 54, and 66 h, making the total concentration of 40 mM in the reaction assay. Similarly, fresh enzymes were added at 16, 30, and 42 h, to maintain the enzyme reaction during the fed-batch reaction. One milliliter of 2.0 M sucrose was also added at 22 and 36 h, to ensure the supply of UDP-α-D-glucose. As a result, the final volume of the reaction assay was 40 mL. The reaction was stopped by denaturing the enzymes by keeping the reaction mixture in boiling water for 5 min. After that, the mixture was centrifuged at 12,000 rpm (13,475×g) for 15 min.

Biosynthesis of quercetin rhamnoside

Regular reaction using TDP-rhamnose

The reaction assay was set up using 3 mM TDP-rhamnose, 1 mM quercetin, 10 mM $MgCl_2 \cdot 6H_2O$, 200 mM Tris-HCl, and 1.0 μg/mL AtUGT89C1 enzyme, making a 200 μL total volume. The reaction mixture was incubated at 37 °C for 20 h.

Cascade reaction for quercetin rhamnoside biosynthesis starting from sucrose

First of all, rhamnoside formation reaction with quercetin was carried out by using 3 mM TDP, 1 mM quercetin, 3 mM NAD$^+$, 3 mM NADPH, 10 mM $MgCl_2 \cdot 6H_2O$, 200 mM Tris-HCl, and 300 mM sucrose; and enzymes AtSUS1 (2.0 μg/mL), AtUGT89C1 (1.0 μg/mL), and AtRHM1 (1.0 μg/mL) were used in the ratio 2:1:1 by concentration. The reaction mixture was kept at 37 °C for 20 h. To explore the best conversion of quercetin to its rhamnoside, ADP, CDP, GDP, and UDP were used, under a similar set of condition as described above.

Analytical methods

In vitro reaction mixtures were directly analyzed by using an RP-HPLC-PDA connected to a C18 column (Mightysil RP-18 GP (4.6 × 250 mm, 5 μm) (Kanto Corporation, Oregon)). The UV used to quantify the naringenin glucosides products was 280 nm. For quercetin reaction, 340 nm was used. HPLC was performed using a binary condition of H_2O (0.1% trifluoroacetic acid buffer) and 100% acetonitrile (ACN) at a flow rate of 1 mL/min for 30 min. The ACN concentrations were as follows: 10, 20, 40, 70, 90, 50, and 10%, for 0–5, 5–10, 10–15, 15–22, 22–25, 25–30, and 30–35 min, respectively. The products were quantified by a calibration curve of authentic standard substrate naringenin created using 0.625, 1.25, 2.5, 5, 10, and 20 μM concentrations. The exact mass of products was analyzed using high-resolution quadruple time-of-light electrospray ionization mass spectrometry (HR-QTOF-ESI/MS) [ACQUITY (UPLC, Waters, Milford, MA)-SYNAPT G2-S (Waters)] in the positive ion mode.

The compounds were purified using a preparative-HPLC equipped with a C18 column [YMC-Pack ODS-AQ (250 × 20 mm I. D., 10 μm)] connected to a UV detector (280 nm) under a binary condition of H_2O (0.05% trifluoroacetic acid buffer) and 100% ACN at a flow rate of 10 mL/min for 35 min. The ACN concentrations were 20, 50, 70, 90, 50, and 20%, for 0–5, 5–10, 10–15, 15–25, 25–30, and 30–35 min, respectively. The purified product was concentrated using a rotary evaporator, followed by lyophilization. The concentrated and completely dried sample was dissolved in D_2O, and dried in a freeze drier, then again dissolved in DMSO-d_6 for nuclear magnetic resonance (NMR) analyses. The compounds were further characterized with a 700 MHz Avance II 900 Bruker BioSpin NMR spectrometer (Germany) using a Cryogenic TCi probe (5 mm). One-dimensional NMR (^{1}H-NMR, ^{13}C-NMR) and two-dimensional NMR (correlation spectroscopy (COSY), nuclear Overhauser effect spectroscopy (NOESY), rotating-frame NOE spectroscopy (ROESY), heteronuclear single quantum correlation (HSQC), and heteronuclear multiple-bond correlation (HMBC)) were

performed to elucidate the structure of the compounds. All the raw data were processed by using TopSpin 3.1 software (Bruker), and further analyzed by using MestReNova 8.0 software (Mestrelab Research S. L., Spain).

Water solubility determination

In order to determine the solubility of naringenin and its glucoside derivatives in the reaction mixture, two sets of reactions were carried out in 500 μL of the reaction mixture. In the first set of reactions, the denatured protein was used, while another set of reactions was used as a regular cascade reaction, as mentioned above. After incubation at 37 °C for 20 h, the reaction mixtures were mixed with the same volume of ethyl acetate, vortexed for 10 min, and then centrifuged, to divide it into two layers. The fractions of substrate and products present in each water and solvent (ethyl acetate) layers were directly analyzed using HPLC, as described previously.

Results

Protein expression and SDS-PAGE analysis

To produce soluble recombinant proteins for in vitro reaction, four plasmids pET28a-YjiC, pET32b-AtRHM1, pET41b-AtUGT89C1, and pQE30-AtSUS1 (Fig. S1 of the Supplementary information) were transformed into *E. coli* BL21 (DE3) host. The SDS-PAGE analysis of a soluble fraction of each protein YjiC, AtSUS1, AtRHM1, and UGT89C1 showed clear bands at around 46, 88, 73.7, and 47.96 kDa, respectively (Fig. S2). The band size corresponds to the calculated molecular weight of each protein with the hexahistidine-tagged fusion protein. The soluble lysate of these proteins was then subjected to Ni^{++}-NTA beads purification system. The purified proteins were concentrated, quantified, and used for in vitro reactions.

Glucosylation of naringenin by YjiC

The reaction mixture of naringenin with UDP-α-D-glucose and YjiC was first analyzed by RP-HPLC-PDA. The chromatograms showed major three different peaks at the retention time (t_R) of 7.86, 10.03, and 10.20 min for P1, P2, and P3, respectively (Fig. 2a(i)). The UV-VIS analysis of novel peaks resembled the naringenin with a subtle difference in pattern (Fig. 2b). The same sample was subjected to high-resolution QTOF-ESI/MS analysis, and observed the exact mass $[M + H]^+$ m/z^+ of P3 as 435.1278, which resembles the single glucose conjugated naringenin. The calculated mass of single sugar conjugated naringenin with the formula $C_{21}H_{23}O_{10}^+$ in the protonated form $[M + H]^+$ m/z^+ was 435.1291 (Fig. 2c(ii)). Likewise, P2 showed the exactly similar mass spectrum $[M + H]^+$ m/z^+ as P3 of 435.1311, indicating the attachment of single glucose with naringenin (Fig. 2c (iii)). Also,

for the product P1, the mass $[M + H]^+$ m/z^+ was 597.1821, which resembled the mass of two glucoses conjugated in naringenin, for which the chemical formula $C_{27}H_{33}O_{15}^+$ with exact mass was 597.1819 (Fig. 2c(iv)). The overall conversion of naringenin to glucosides was about 94%.

Cascade reaction using sucrose synthase and glucosyltransferase

To generate an efficient, cost-effective, and sustainable biocatalytic synthesis of naringenin glucosides, we coupled naringenin glucosylation reaction catalyzed by YjiC with UDP-α-D-glucose synthesizing sucrose synthase AtSUS1 enzyme. In the presence of UDP, AtSUS1 hydrolyzed sucrose to produce UDP-α-D-glucose and fructose as a by-product. Thus the produced UDP-α-D-glucose is eventually utilized by YjiC to transfer glucose moiety to naringenin (Fig. 1a, b).

The cascade reaction was carried out as described in the "Materials and methods" section. The samples collected from the reaction vessel at different time points of 3, 6, 10, and 20 h were analyzed by RP-HPLC. The chromatograms were compared with the results from regular glucosylation reaction (Fig. 2a(ii)), the standard naringenin, and the control reaction (Fig. 2a). All the three peaks were produced in the reaction, which showed the efficient formation of UDP-α-D-glucose and recycling of UDP after glucosylation reaction. The concentration of P1 and P3 increased from 3 to 20 h, while that of P2 decreased gradually (Fig. S3). Importantly, almost 95% of the initially added 5 mM naringenin was converted into products.

Optimization of cascade reaction

To optimize the cascade reaction of naringenin glucosylation using AtSUS1 and YjiC, we performed a series of reactions under different conditions, by varying the enzymes ratio, donor and acceptor substrates concentration, temperature, buffer, and divalent metal ions.

Enzymes concentration variation

To identify the bottleneck for the combined enzymatic reactions, the concentration of two enzymes used in the reaction was varied, and the outcome of the reaction was closely monitored for the optimal conversion of naringenin. As expected, a different pattern of product profile was obtained while varying the enzyme ratio in the cascade reaction. With the 1:5 and 1:10 ratios of enzymes YjiC:AtSUS1, the exactly similar pattern of the peaks P1, P2, and P3 were found, P1 being in the largest abundance, followed by P2, and then P3. But while decreasing the ratio of YjiC and AtSUS1 gradually to 1:1 and 1:2, the products peaks were fluctuating. The peak P2 was more prominent in the ratios 1:1 and 1:2 (Fig. 3a). In the ratio 10:1 between YjiC and AtSUS1 enzymes, P1 was found to be more dominant, while P2 was least
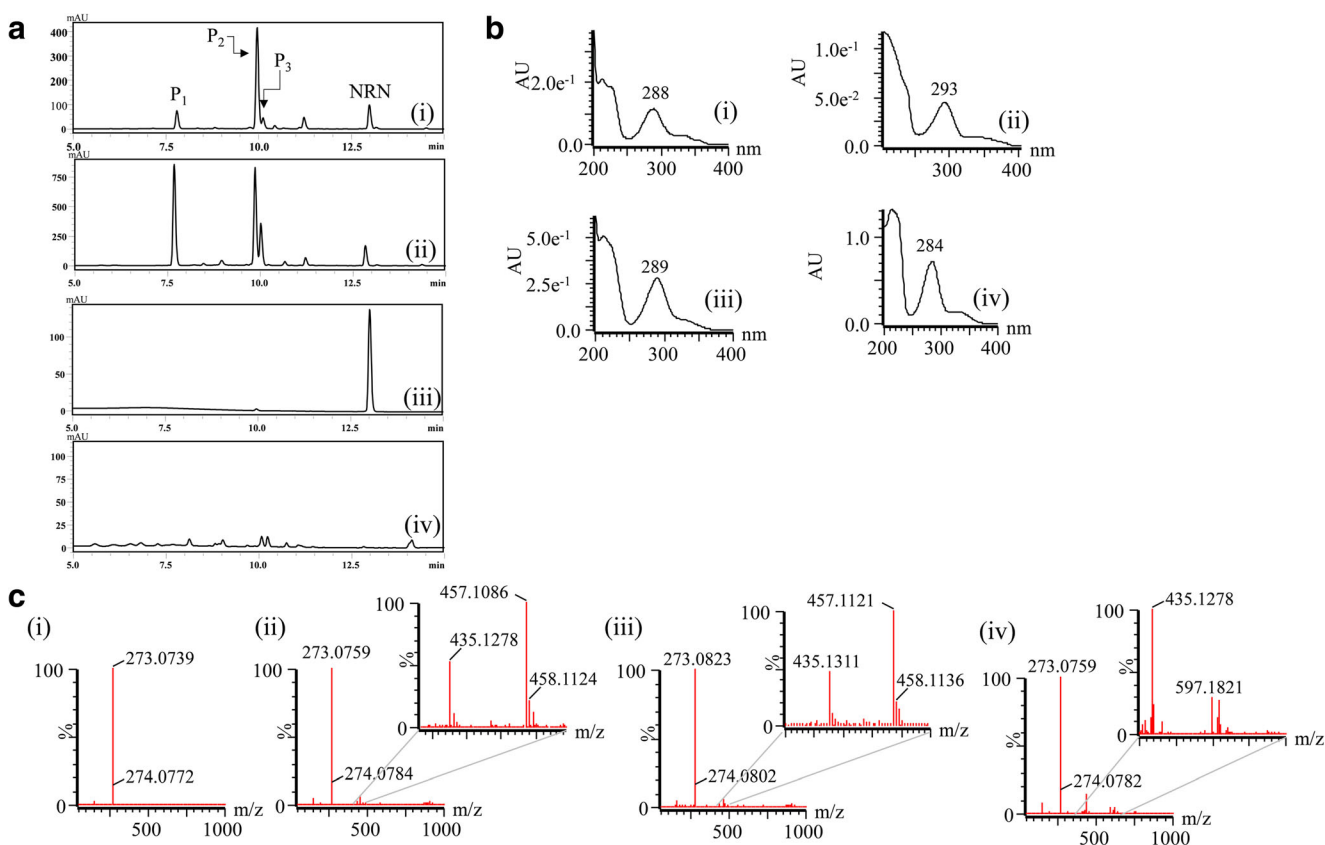
Fig. 2 **a** HPLC analysis of naringenin (NRN) reaction mixture. (i) Regular glucosylation reaction carried out using YjiC, (ii) cascade reaction using AtSUS1 and YjiC enzymes at 10 h, (iii) standard naringenin; and (iv) control reaction for cascade reaction. **b** UV-VIS analysis of each peak from HPLC. (i) Standard naringenin, (ii) P_1, (iii) P_2, and (iv) P_3. **c** HR-QTOF-ESI/MS analysis. (i) naringenin standard, (ii) P_1, (iii) P_2, and (iv) P_3

among all other. Depending upon the types of product requirement, the ratio of the enzymes could be varied. Moreover, the conversion percentage of naringenin to glucosides was not significantly altered by changing the ratio of enzymes.

Optimization of UDP-α-D-glucose concentration

Six sets of experiments were carried out with changing the concentrations of UDP-α-D-glucose from 0.1 to 1.0 mM, keeping all other reaction components constant. The result showed P1 and P3 as a prominent product in all the UDP-α-D-glucose concentrations. But when 1.0 mM of UDP-α-D-glucose was used, P2 was also abundantly present (Fig. 3b). The conversion of naringenin was about 89.70% when 0.1 mM of UDP-α-D-glucose was used, which was 5–6% below that in other reactions. This result showed an efficient supply of UDP-α-D-glucose for the glucosylation reaction, despite the variation in concentration of initial concentration. For further reactions, 1.0 mM of UDP-α-D-glucose was used.

Naringenin substrate tolerance

Four sets of identical reactions were carried out at various naringenin concentrations (5, 8, 10, and 12 mM) to one-pot

two-enzyme reaction system containing AtSUS1 and YjiC in the ratio of 1:10 (YjiC:AtSUS1), keeping the other components fixed. The product formation and substrate conversion were monitored after 20 h. The HPLC showed a predominant product peak P2 at the concentration of 8, 10, and 12 mM. At 5 mM concentration of naringenin, other product peaks also appeared with decreasing concentration from P1 to P3 (Fig. 3c).

When 5 mM of naringenin was used as an acceptor substrate, the conversion of naringenin was approximately 96%. When the concentration was increased, the conversion percentage was decreased. At 12 mM naringenin concentration, the conversion was only about 44.21% which was much lower (32.88%) when 8 mM of naringenin was used. Thus, 5 mM of naringenin was selected for further experiments.

Effects of temperature variation

The results obtained in the different ranges of temperature from 4 to 60 °C showed multiple impacts in the product formation (Fig. 3d). At 4 and 60 °C, only two products P1 and P2 formed out of the three products, whereas at 20 and 50 °C, three products P1, P2, and P3 formed. The products P1 and P2 were formed in all the ranges of temperature aforementioned, while product P3 was formed
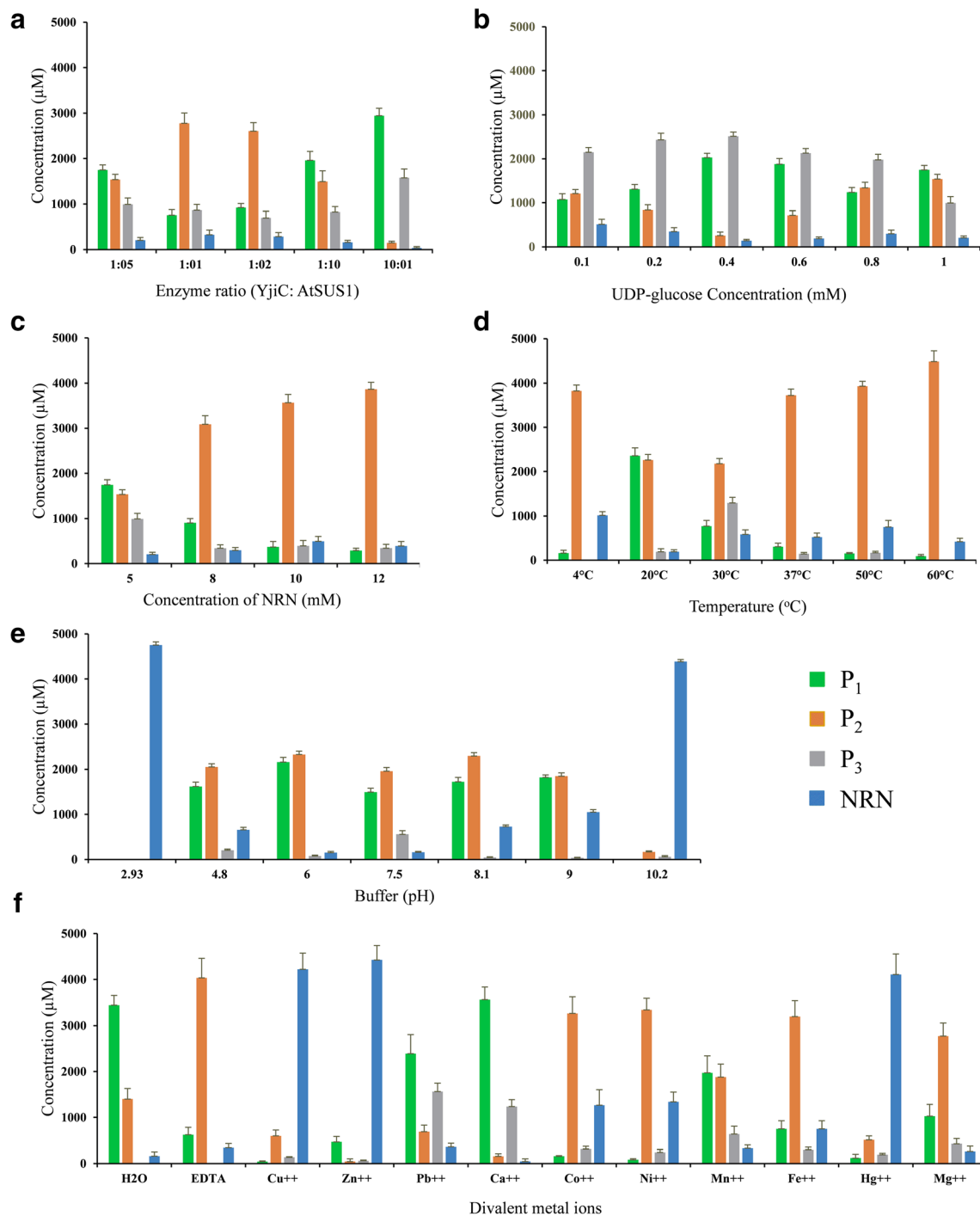
Fig. 3 Cascade reaction optimization for naringenin glucoside biosynthesis starting from sucrose. **a** Enzyme concentration variation, **b** variation of starting concentration of UDP-glucose, **c** variation of starting concentration of naringenin (NRN), **d** reaction at different temperatures, **e** reaction in different buffer with different pH, **f** effects of metal ions

only at 20 to 50 °C. The reaction temperature has multiple impacts: high specific activities at high temperatures, enzyme deactivation, and metabolite degradation (Myung et al. 2009). The amounts of formation of all products at 37 °C were found to be more prominent than at 30 °C. Therefore, the optimal reaction temperature was 37 °C.

Effects of buffer variation

To find out the optimal pH for the reaction assay, the glucoside production was investigated at 37 °C, keeping all other reaction ingredients intact, and varying the buffer and pH. The pH of the different sets of the reaction was adjusted from 2.93 to

10.2 in 100 mM of acetate, phosphate, Tris-HCl, and glycine buffer with their respective pH as mentioned in the "Materials and methods" section. The reaction was monitored after incubating at 37 °C for 20 h. The result showed that at low pH 2.93, none of the product peaks formed (Fig. 3e). At pH 10.2, the substrate was found to have reacted very little, and only a few products peaks were formed. The enzyme showed good activity in the pH 4.8 to 9 with different buffers. The conversion of the substrate was highest at pH 6 and 7.5, but the product's distribution was different at all pH. Therefore, the optimal pH for the reaction was 7.5, as all the product formation at pH 7.5 was found to be measurable enough, and dominant under the reaction conditions.

Effect of metal ions

In the presence of different divalent metal ions, the maximum conversion of naringenin occurred with calcium ions, and least with zinc ions. Similarly, a significant amount of products were formed with deionized water, as well as chelating agent EDTA, which could further suggest that the enzymes used might not be affected by the metal ions or independent with divalent metal ions. However, the presence of some divalent metal ions, such as Cu^{2+}, Zn^{2+}, and Hg^{2+}, showed a detrimental effect on the enzyme reaction (Fig. 3f).

Preparative scale production of NRN glucosides

While analyzing the product profile at different time points, three distinct peaks were initially observed. Among them, the peak at t_R 10.03 min (P2) was initially the most dominant, but with increasing incubation time, peaks at t_R 7.86 min (P1) and 10.20 min (P3) significantly increased, while that of P2 gradually decreased. After incubation more than 16 h, new peaks at t_R 8.35, 8.82, and 10.83 min for P4, P5, P6, and P7, respectively, began to appear, and became prominent after 42 h (Fig. 4, and Fig. S4). The peak (P1) at t_R 7.86 min became the largest after 60 h. On the basis of the nature of the formation of the product, the amount of desired products can be controlled by changing the incubation periods of the reaction. As time increases, the nature of mono-glucosylated products changes into di-glucosylated product. The mono-glucosylated products were found at t_R 10.03 min and 10.20 min and the di-glucosylated product was found at t_R 7.86 min (Fig. 2, and Fig. S4). During the reaction, it was found that the conversion of the substrate, naringenin, into its products was 94.66 to 89.05%, while analyzing the spectrum obtained from the incubated reaction samples from 10 to 76 h in the different intervals by RP-HPLC. Since the scale-up reaction is a fed-batch process, with the addition of fresh enzymes, donor, and acceptor, the rate of conversion was observed fluctuating. The RC_{max} value during the reaction is 20.10. The calculated regular products at 76 h are P1, P2,

and P3 at 30.88, 23.475, and 18.35%, and additional unknown products were found as P4, P5, P6, and P7 at 4.48, 3.27, 5.34, and 2.75% respectively (Fig. 4; Figs. S4 and S5).

Structure elucidation

All the peaks seen in preparative scale reactions were purified using prep-HPLC. The purity of each compound by HPLC analysis was above 98% (Fig. 5). The purified compounds were dried using a rotary vacuum evaporator, followed by lyophilization for NMR samples prepared as described in the "Materials and methods" section. The HR-QTOF-ESI/MS analysis of peaks P1, P2, and P3 clearly indicates for product P1 the presence of two glucose molecules in naringenin, while P2 and P3 have single sugar conjugated mass. But the masses of peaks P4, P5, P6, and P7 were found to be 880.24259, 503.17915, 517.1948, and 356.14925 Da, respectively.

^{1}H-NMR analysis of P1 shows the absence of two proton peaks at chemical shift value δ 10.81 ppm (7-OH) and δ 9.61 ppm (4′-OH), meaning two glucoses are conjugated at 7- and 4′-OH positions of naringenin. The presence of two anomeric proton peaks at δ 4.88 ppm (d, J = 7.7 Hz) and δ 4.94 ppm (d, J = 7.8 Hz) further confirmed two glucose units in the beta configuration. Other peaks for glucose and naringenin were present at δ 3.15–3.80 ppm and δ 5.5–7.5 ppm, respectively (Fig. S6). Similarly, in ^{13}C-NMR analysis, two anomeric carbon peaks appeared at δ 99.97 ppm and 100.56 ppm. Other carbon peaks were present in between δ 60 and 80 ppm (Fig. S7). The detail ^{1}H- and ^{13}C-NMR data are presented in Table S1 and S2. These data were further supported by ^{1}H-^{1}H COSY, HSQC-DEPT + HMBC, ROSEY, HSQC-DEPT, and HMBC NMR analyses (Figs. S8-12). The correlations between different protons, as well as between protons and carbons, are presented in the respective figures in supporting data. All these analyses clearly elucidated the structure of the product P1 as naringenin, 4′, 7-O-β-D-diglucoside. In the elucidated structure of the naringenin, 4′, 7-O-β-D-diglucoside, chiral carbon present at the 2-C position of naringenin backbone, and as a result, there is the formation of a mixture of R and S conformation compounds, which is supported by the clear presence of additional carbons and protons peaks in the spectrum.

Likewise, in analyzing the ^{1}H-NMR of P2, there is absence of the 7-OH position's peak having a chemical shift δ 10.81 ppm, and the presence of peaks in the sugar region of δ 3.15–3.80 ppm along with naringenin at δ 5.5–7.5 ppm, which means the conjugation of glucose in the 7-OH position of naringenin (Fig. S13). Furthermore, this conjugation is supported by the presence of one anomeric proton peak at δ 4.99 ppm (d, J = 7.77 Hz). Likewise, with ^{13}C-NMR analysis of P2, there is the presence of one anomeric carbon peak at δ 100.06 ppm, and the rest of other carbons of naringenin in the region δ 80–180 ppm and carbons of sugar in δ 60–80 ppm

Fig. 4 Fed-batch preparative scale cascade reaction. **a** Biosynthesis of naringenin glucosides at different time intervals. **b** Conversion percentage of naringenin (NRN) at different time points (* denotes addition of naringenin and # denotes addition of fresh enzymes and sucrose to the fed-batch system)
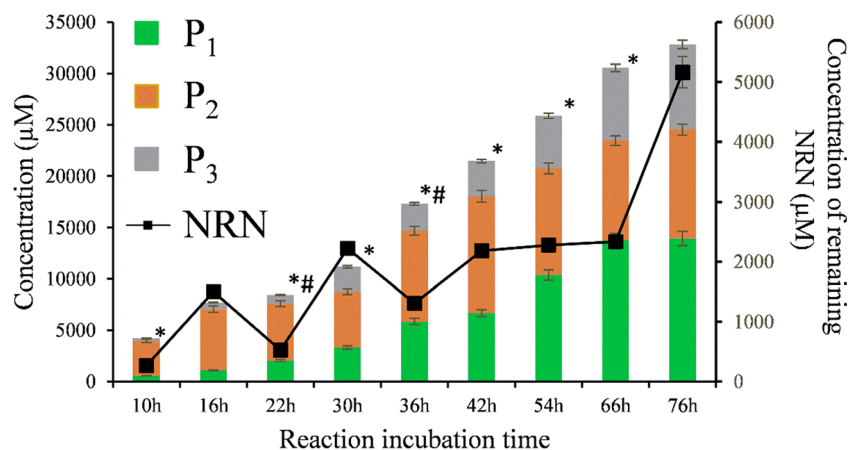
(Fig. S14). Tables S1 and S2 present the detailed ^{1}H- and ^{13}C-NMR data. The exact structure of the P2 was further supported by the correlation between different protons, and protons-carbons obtained by the analysis of the ^{1}H-^{1}H COSY, HSQC-DEPT + HMBC, ROSEY, HSQC-DEPT, and HMBC (Figs. S15-19). With all this evidence, the product P2 is identified as naringenin, 7-O-β-D-glucoside.

The product P3 is characterized as naringenin, 4′-O-β-D glucoside with the 1D as well as 2D-NMR analysis of ^{1}H-,^{13}C-, ^{1}H-^{1}H COSY, HSQC-DEPT + HMBC, ROSEY, HSQC-DEPT, and HMBC. There is the absence of the proton peak of the 4′-OH position of naringenin at δ 9.61 ppm. The anomeric proton peak appeared at δ 4.90 ppm (d, J = 7.58 Hz), and the presence of sugar proton peaks in the region δ 3–5 ppm (Fig. S20). With ^{13}C-NMR analysis, the anomeric carbon peak obtained at δ 100.72 ppm and other carbon peaks at δ 70–80 ppm justify the presence of one sugar at the 4′-OH position of the

naringenin (Fig. S21). The detail ^{1}H- and ^{13}C-NMR data are presented in Table S1 and S2. The correlation observed in analyzing ^{1}H-^{1}H COSY, HSQC-DEPT + HMBC, ROSEY, HSQC-DEPT, and HMBC, in between different protons and protons-carbons, also further supports the conjugated position of sugar with naringenin (Figs. S22-26).

The additional peaks (P4, P5, P6, and P7) produced during the late stage of long incubation of the scale-up reaction were collected as impurities. HR-QTOF-ESI/MS analysis of those peaks has shown the masses of 881.24259, 503.17915, 517.19480, and 356.14925 Da, respectively. Since the mass number is unique and does not match with the naringenin, we further isolated each compound in pure fraction, and performed various NMR analyses.

The HR-QTOF-ESI/MS analysis of P4 showed the unique mass fragments as [M + H]$^+$ m/z^+ 881.249 as the parent ion peak, and (719.1974, 557.1422, 447.1248, 285.0739) as

Fig. 5 HPLC chromatogram of purified compounds from the preparative reaction mixture. **a** Chromatogram of the crude reaction mixture. **b** Chromatograms of prep-HPLC purified compounds
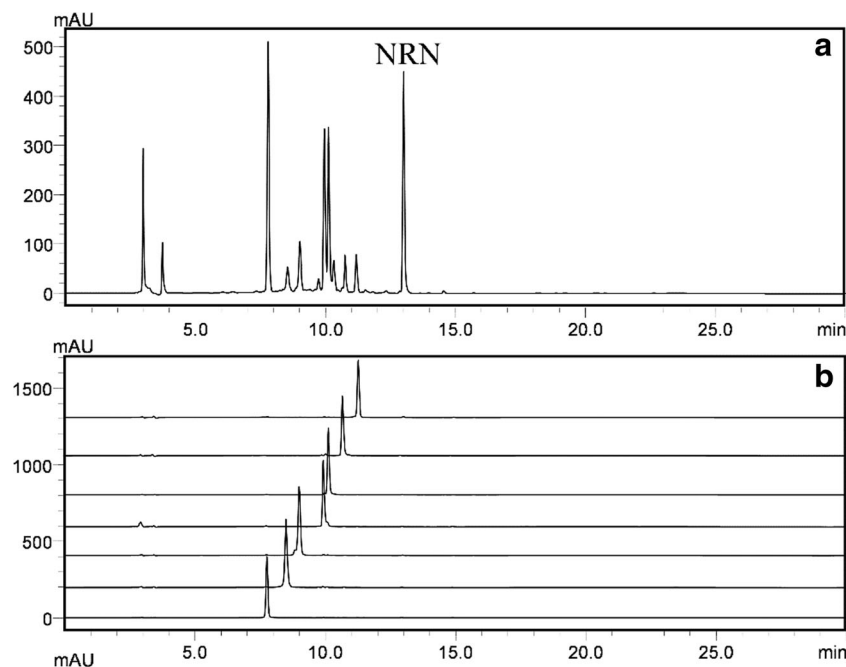
fragment ion peaks (Fig. S27). The mass difference between the first three mass peaks [881–719, 719–557] was the difference of 162 amu, which confirmed conjugation of two glucose units in an aglycon of mass 557.1422 Da. The successive loss of glucose unit from a parent molecule resulted in the generation of a mass fragment of single glucose conjugated 719.1974 Da and aglycon of mass 557.1422 Da. The observed mass pattern of 881.2494 Da suggests the possible structure of P4 might be double glucose moieties attached to the dimer of naringenin and the mass 557.5242 Da as aglycon, a dimer of naringenin itself, since these masses were matched with their exact masses of 881.2504 and 557.1448 Da, respectively.

Further, the ^{1}H-NMR and ^{13}C-NMR analyses provided supporting evidence to predict the possible structure as a diglucoside of a dimer form of naringenin connected with a methylene linkage at C-6 position, as proton peaks and carbon peaks were obtained with the double number, and the 6-H proton is missing (Tables S1 and S2, Figs. S28 and S29). This provides the solid information that there is linkage at C-6 of naringenin. While analyzing 1D as well as 2D-NMR spectra, the correlation obtained in different protons along with carbons and protons through the analysis of ^{1}H-^{1}H COSY, HSQC-DEPT + HMBC, ROSEY, HSQC-DEPT, and HMBC clearly identified the position of sugars and the P4 product as a di-4′-O-β-D-glucoside naringeninyl methylene with a methylene linker at C-6 position as shown in Figs. S30-34 of the Supporting Information.

In the same way, various NMR analyses were conducted for the peak P5, which also has unique mass value [M + H]$^+$ m/z^+ value as 504.1866 (Fig. S35). The ^{1}H-NMR analysis showed an anomeric peak at chemical shift value δ 4.89 ppm (dd, J = 7.81 Hz), along with other peaks for a glucose moiety in between δ 3.0 and 3.7 ppm. The proton peaks also showed spectra resembling naringenin backbone. However, the absence of 6-H proton and the presence of additional proton peaks between δ 8.1–9.3 ppm and δ 1.5–3.3 ppm provided a hint that an additional group is attached at the C-6 position. The 2D-NMR analyses along with ^{1}H- and ^{13}C-NMR analyses and ESI/MS analysis led to the identification of P5 as 6-(2-pyrrolidinyl) naringenin, 4′-O-β-D-glucoside (Tables S1 and S2, Figs. S36-42).

Similarly, P6 showed a unique mass of [M + H]$^+$ m/z^+ 518.2029, which is just 14 amu greater than P5 in the HR-QTOF-ESI/MS mass analysis (Fig. S43). A prominent mass fragment peak of 356.1489 Da appeared, which is just exactly 162 amu lower than the parent peak. This gives the clue that the peak is a glucosylated derivative of an aglycon with the mass of 356.1489 Da.

Similar to P5, the almost analogous pattern of peaks appeared in ^{1}H-NMR, with almost similar chemical shifts. However, additional peaks appeared in the range of δ 1.5–3.5 ppm (Fig. S44). The detailed analysis of all available 1D-NMR and 2D-NMR led to the identification of P6 as a

6-(2-piperidinyl) naringenin, 4′-O-β-D-glucoside. The detailed correlation studies between different protons and protons-carbons are presented in supporting data in their respective places, whereas Tables S1 and S2 present the detailed ^{1}H- and ^{13}C-NMR data, and Figs. S45-51 represent all 2D-NMR analyses information.

Another new peak appeared during the long incubation of the large-scale reaction mixture, namely P7, showed the exact mass as [M + H]$^+$ m/z^+ 356.1490. This mass exactly matched to the aglycon part of P6, suggesting the possible piperidine conjugated with naringenin at the 6-C position. However, the NMR data surprised us, during analyzing P4. Thus, we further analyzed P7 by various 1D as well as 2D NMRs. The ^{1}H-NMR spectra exactly resembled the aglycone part of P6, as shown in Fig. S52. The proton peaks of naringenin backbone along with the proton peaks of piperidine in the region of δ 1.5–3.5 ppm supported the mass of the predicted C-6 piperidine conjugated naringenin (Table S1). There were no peaks of sugar protons (Fig. S53). Further, analysis of ^{13}C-NMR obtained the carbons peaks that also matched the aglycon part of P6 (Table 2, Fig. S54). However, we performed further 2D-NMR analyses to verify the structure, by studying the correlations between protons and carbons. Finally, with the correlation obtained in between different protons, along with the carbons and protons through the analysis of ^{1}H-^{1}H COSY, HSQC-DEPT + HMBC, ROSEY, HSQC-DEPT, and HMBC, we clearly identified the structure of the P7 as 6-(2-piperidinyl) naringenin (Fig. S55-60).

Further, the Sci-finder chemical library was used to check the novelty of the additional peaks. The product P7 is deposited in the Library [CAS registry 2125981-78-2]. The IUPAC name of this compound is [4H-1-Benzopyrane-4-one-2, 3-dihydro-5, 7-dihydroxy-2-(4-hydroxyphenyl)-6-(2-piperidinyl)]. But the others (P4, P5, and P6) are not listed in the library. However, P1, P2, and P3 are listed in the library under a different CAS registry number. Figure S61 presents the structures of all the impurities present in the standard naringenin sample and the glucoside derivatives of the impurities.

Since we were surprised with the unexpected molecules (P4-P7) isolated from the reaction mixture, we suspected the standard naringenin as the source of these compounds. Thus, standard naringenin was further analyzed by HR-QTOF-ESI/MS. The mass analysis showed the presence of all three aglycone compounds ((Di-6-naringeninyl) methylene, 6-(2-pyrrolidinyl) naringenin, and 6-(2-piperidinyl) naringenin) in the standard sample (Figs. S62-64) in trace amounts. The YjiC enzyme accepted these impurities as acceptor substrate, and eventually lead to the production of glucosylated derivatives, since the fed-batch addition of naringenin in the large-scale reaction mixture led to the accumulation of these impurities in significant amount, which was ultimately isolated as pure compound, and identified by various NMRs.

Reaction assay with NDPs

To study the influence of product profile using five different natural nucleotide diphosphates (ADP, CDP, GDP, TDP, and UDP), the reactions were carried out as mentioned in the "Materials and methods" section. These NDPs were used in the reaction, instead of UDP-α-D-glucose. Thus, AtSUS1 first synthesizes NDP-glucose from sucrose, which is utilized by YjiC, eventually to form glucosides of naringenin. The three types of glucosylated products were observed in the HPLC analysis of all reaction samples. However, the lowest conversion of naringenin to glucosylated products was observed with GDP among all. Among five NDPs, the highest conversion of naringenin was found with UDP. The highest conversion percentage was found to be 77.81% with UDP, followed by 74.99% with CDP (Fig. 6).

Biosynthesis of quercetin rhamnoside using sucrose as a source of rhamnose

Regular rhamnosylation reaction

After successful optimization and synthesis of practical quantities of naringenin glucosides from sucrose as the primary source of glucose, we extended the system for the biosynthesis of rhamnoside derivative. For this, a rhamnosyltransferase UGT89C1 and a UDP-β-L-rhamnose synthase (AtRHM1) were used along with AtSUS1. All three enzymes from *A. thaliana* were overexpressed and produced in *E. coli* BL21 (DE3), purified, and used for the production of quercetin 7-O-rhamnoside.

In the beginning, the reaction was carried out with quercetin and TDP-rhamnose, to check if overexpressed enzyme UGT89C1 reacts with both donor and acceptor substrates. The HPLC analysis revealed the production of a distinct peak at t_R 10.5 min (Fig. 7a). The peak was further confirmed to be quercetin rhamnoside by UV absorbance (Fig. 7b), and the protonated mass of 449.1079 Da by HR-QTOF-ESI/MS

analysis (Fig. 7c). Since the UGT89C1 enzyme is well known to conjugate rhamnose at the 7-OH position by previous studies (Yin et al. 2014; Kim et al. 2013), we did not further characterize the product by NMR analysis.

Reactions with NDPs for quercetin 7-O-rhamnoside biosynthesis

One-pot three enzymes (AtSUS1, AtRHM1, and AtUGT89C1) were used with quercetin and TDP for rhamnosylation of quercetin, starting from the biosynthesis of TDP-L-rhamnose using sucrose. The HPLC chromatogram obtained after the reaction showed that there is a formation of quercetin 7-O-rhamnoside product at exactly the same time in the HPLC profile (Fig. S65).

We also studied the effect of different NDPs on the formation of quercetin 7-O-rhamnoside product under similar condition, and compared the substrate conversion with the product (Fig. S65). In the presence of GDP, almost 50% of quercetin was converted into a product that was below 30% with UDP and about 20% with other NDPs (Fig. 7d). During NDP-L-rhamnose biosynthesis from sucrose, NDP-glucose is produced as an intermediate stable metabolite in the reaction, which could be utilized by UGT89C1 to transfer at 3-OH of quercetin. Thus, to confirm the specificity of UGT89C1 towards different NDP-sugar donors, we also carried out the reaction with UDP-α-D-glucose and quercetin. However, we did not observe any product in HPLC-PDA analysis (Fig. S66). The enzyme also did not accept flavanone such as naringenin as acceptor substrate while using UDP-α-D-glucose as a donor substrate.

Water solubility determination

The glycoside derivatives of naringenin were found more in the aqueous layer than in an organic phase. The glucosylated derivatives were mostly located in the aqueous phase, and were little extracted from the ethyl acetate layer, while the
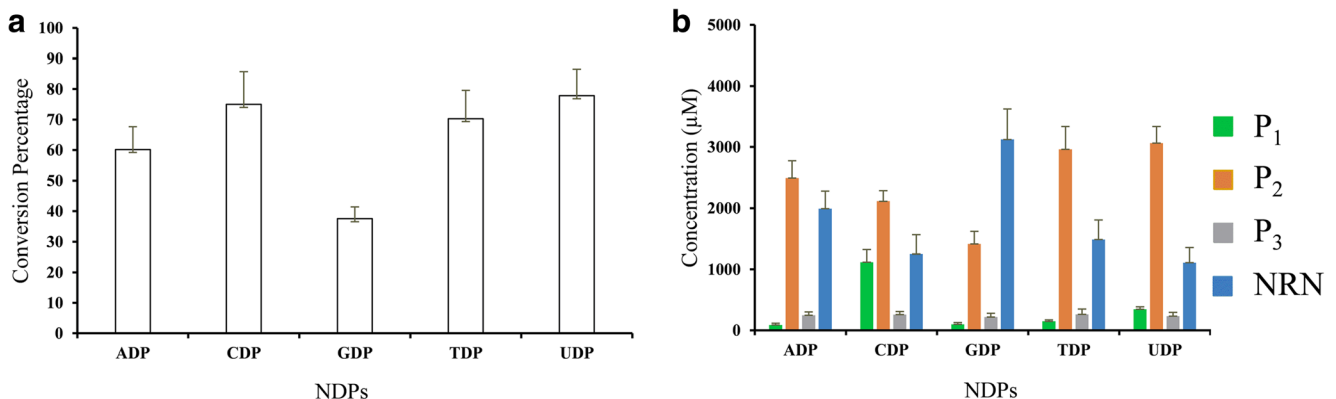

Fig. 6 Conversion of naringenin to glucosides in the cascade reaction system using different NDPs. **a** Conversion percentage of naringenin, **b** production of different glucosides
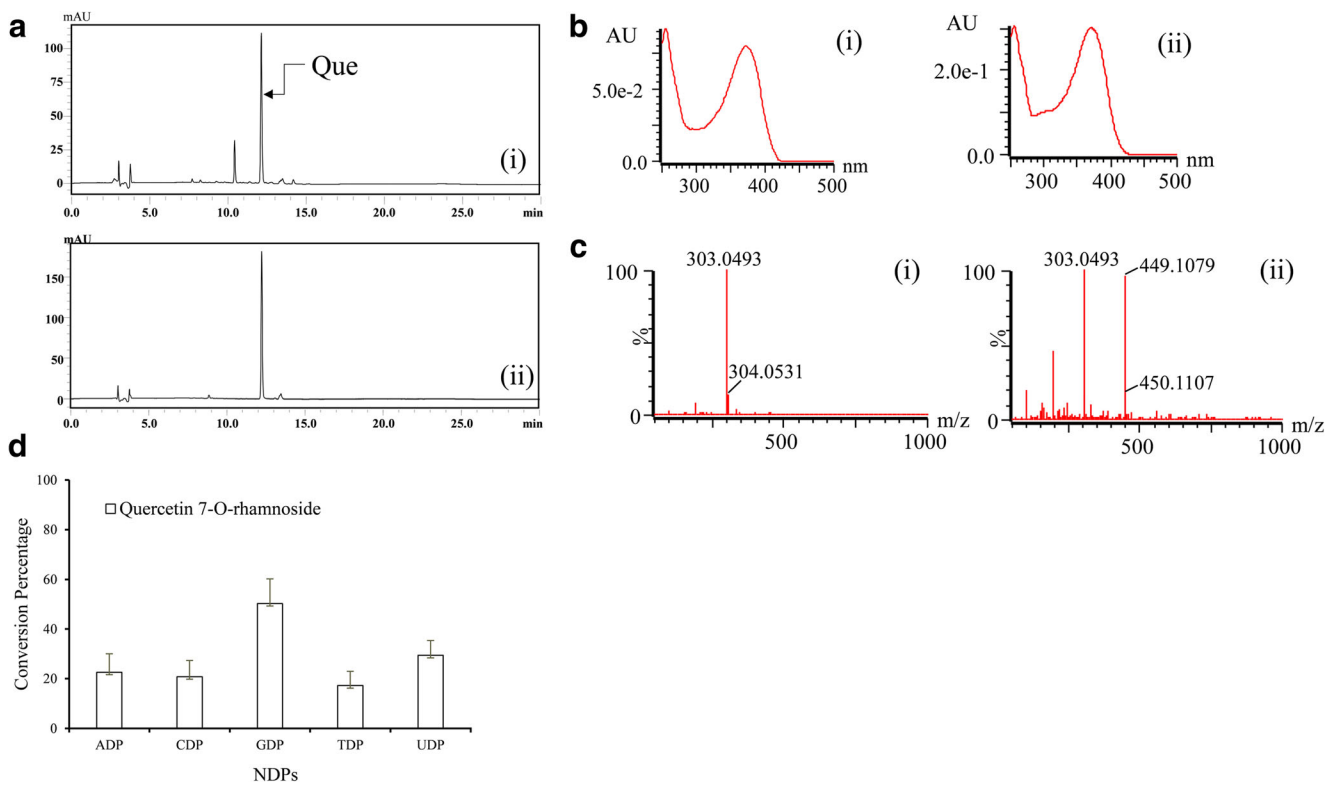
Fig. 7 Reaction analysis (**a**) HPLC chromatogram of (i) UGT89C1 reaction with quercetin and TDP-rhamnose and (ii) UGT89C1 reaction with UDP-glucose and quercetin. **b** UV/VIS analysis of (i) quercetin standard and (ii) reaction product, quercetin 7-O-rhamnoside. **c** HR-QTOF-ESI/ MS analysis of (i) quercetin and (ii) reaction product. **d** Biosynthesis of quercetin rhamnoside using cascade reaction system (AtSUS1, AtRHM1, UGT89C1) starting from the sucrose in the presence of five different NDPs

substrate compound, naringenin, preferred to remain in ethyl acetate fraction, more than in water fraction because of the less effective hydrogen bonds formation as there is less hydroxyl (–OH) groups present in naringenin compared with its glucosides. The water solubility of naringenin glucoside was higher by approximately 5.4-fold than naringenin. Therefore, the glycosylated compounds have significantly improved water solubility in comparison with naringenin (Fig. S67).

Discussion

Researchers have focused on the effective production, maximum utility, and bioactivities of various types of natural flavonoids. But due to the limitation of their water solubility and amount availability from natural sources, there are challenges associated with the production and supply of target flavonoids. To overcome such difficulty, modification of natural flavonoids is done by conjugating bulky hydrophilic groups, such as glucose, galactose, glucuronic acids, and rhamnose moieties, so that modified compounds would make more effective hydrogen bonding with water molecules, thus enhancing their water solubility. Furthermore, modifying compounds with other different moieties, such as methyl, acetyl, hydroxyl,

halides, nitro-, and different types of sugars, not only helps to diversify natural flavonoids but also makes them more efficient as medicinal or cosmetic compounds (Koirala et al. 2014; Antonopoulou et al. 2016; Deng et al. 2017; Teles and Souza 2018). Despite existing different methods of making glycosylated flavonoids, here we make glycosylated flavonoids using a cheap and sustainable recycling system, with sucrose as the main source of sugar moieties. During the process, we used sucrose synthase AtSUS1, rhamnose synthase AtRHM1, and rhamnosyltransferase UGT89C1 from *Arabidopsis thaliana*, and a glycosyltransferase YjiC from *Bacillus licheniformis* DSM 13. We employed these four enzymes produced in *E. coli* to develop two independent systems that produce glucosylated naringenin derivatives and rhamnosylated quercetin. Both sugar moieties are derived from the same source sucrose.

In previous studies, glucosides of quercetin, resveratrol, and apigenin were reported by using the same enzyme, sucrose synthase AtSUS1 and UGT73A15 in the presence of sucrose (Terasaka et al. 2012; Schmölzer et al. 2016). We report the very efficient system to produce multiple glucoside derivatives of naringenin under optimized conditions of time, temperature, pH, buffer, enzyme ratio, UDP-α-D-glucose, and naringenin concentration, and divalent metal ions. When the

fed-batch reaction was performed in a large concentration of naringenin (40 mM) under optimized conditions as described in the "Materials and methods" section, we observed the efficient conversion of naringenin into glucosides with RC_{max} of 21.10 (Fig. S4).

During the analysis of the products of scale-up reaction for a long time incubation up to 76 h, unusually four more products P4, P5, P6, and P7 were obtained (Fig. S4(x)). Previously, it was thought that all seven peaks were the glucosylated naringenin derivatives, but with the 2D-NMR and HR-QTOF-ESI/MS analysis of each purified peak, these peaks were identified as glucosides of impurities present in the standard naringenin (Figs. S62-64).

On the basis of a chemical library Sci-finder search, the identified compounds P4, P5, and P6 are new compounds that could have high biological and pharmacological activities, and that are yet to be studied. The product P7 is found to be an aglycone of product P6. Figure S61 lists the chemical structure of the impurity compounds.

In our one-pot AtSUS1-GT cascade reaction, just by supplying easily available cheap sucrose as a source of sugar moiety and substrate, naringenin, glucosylated products were obtained in large scale, which could pave the path for the application of this system in industry as a cost-effective, green-approach for the biosynthesis of diverse glucoside products. Though there are several methods of making NDP sugars and flavonoid glycosides, our system is one of the best, based on the recycling of highly expensive NDPs and NDP sugars enzymatically, which not only minimizes cost, process, and time but is also a green and sustainable approach (Gantt et al. 2011; Zhang and Chen 2006). However, there are many glucosylated products that could create difficulties in their purification. Thus the target glucosylated product could be obtained using a specific GT, instead of YjiC.

Even though the production of glucosylated flavonoids is very effective by enzymatically using NDPs sugar (Schmölzer et al. 2017; Yuan et al. 2018; Darsandhari et al. 2018), the use of such sugar is not cost-effective or economically feasible. Therefore, the recycling of NDPs and efficient synthesis of NDP sugars are the most vital to make the system sustainable and highly productive. The formation of glucosylated products using YjiC is limited in the long run due to the high deposition of NDPs, as there is competitive inhibition between similarly structured NDP sugars and NDPs (Fig. 1). Hence, the use of sucrose synthase, AtSUS1, not only helped to make the system economically cheap but also made the process chemically stable and sustainable. The system also reduced the accumulation of NDPs; as a result, the chance of competitive inhibition was minimized one side, but on the other side, the decreased concentration of NDPs supports the movement of the equilibrium system towards the product side, according to Le-Chatelier's Principle. Overall, the system is able to convert more substrates into glucosylated products. In addition, in the optimized system, five different types of NDPs, of ADP, CDP, GDP, TDP, and UDP were used, and the results were analyzed. With UDP, about 77.81% naringenin was converted into its glucosylated products. Hence, as many research reports have revealed that sucrose synthase from bacteria prefers TDP, and sucrose synthase from plants has a preference for UDP (Figueroa et al. 2013; Diricks et al. 2017), here also, AtSUS1 form plant shows more preference for UDP, compared with the others (Fig. 7d).

We further expanded the NDP-α-D-glucose biosynthesis system to an NDP-β-L-rhamnose biosynthesis system by introducing an additional enzyme AtRHM1 from A. thaliana. In the one-pot rhamnosylation assay, sucrose synthase, AtSUS1 hydrolyzes sucrose into NDP-α-D-glucose, and fructose with NDP, which later changes into NDP-β-L-rhamnose by AtRHM1 in the presence of cofactors NAD$^+$ and NADPH (Fig. 1). Finally, glycosyltransferase, AtUGT89C1 accepts NDP-β-L-rhamnose as donor substrates, and transfers rhamnose moiety to quercetin during the reaction assay. Thus, the system produces quercetin 7-O-rhamnoside as a product and NDP as a by-product, which is eventually utilized by AtSUS1 to hydrolyze sucrose in the presence of water, and synthesizes NDP-glucose. Thus, AtSUS1 helps to supply NDP-glucose continuously from the cheap source sucrose. AtUGT89C1 is a well-characterized enzyme to transfer rhamnose at the 7-position of flavonoids, like kaempferol, quercetin, fisetin, myricetin, and morin (Kim et al. 2013; Yin et al. 2014; Parajuli et al. 2015) from UDP-β-L-rhamnose.

There are different approaches for the biosynthesis of quercetin rhamnoside, like microbial biotransformation using different microorganisms (Lee et al. 2008; Xiao et al. 2014). E. coli is also becoming popular in synthetic biology for the efficient cell factories designed by genetic manipulation, or recombining heterologous genetic materials (Shiloach and Fass 2005). Additionally, the use of synthetic vector and heterologous expression of stereo- and regio-specific genes into a single vector has been practicable approaches for the efficient production and modification of secondary metabolites (He et al. 2015). However, there are some limitations, as well as the production of side products, less production of required products, or use of strict conditions and the use of expensive precursor materials in the aforementioned methods. So in order to mitigate the problems that appeared, we developed an in vitro system that utilizes sucrose as a primary source of the sugar moiety. Since the use of NDP-β-L-rhamnose sugar and other NDP sugars is very expensive, the continuous supply of such sugars is the most important during glycosylation reactions, which are performed with the use of sucrose synthase, AtSUS1 and AtRHM1, from very simple and cheap source, sucrose, by using the recycling system of NDPs. The best part of this approach is to just supply substrate and sucrose with the addition of fresh enzymes if necessary, for the scale-up production of rhamnoside products.

In conclusion, one-pot two-enzyme or three-enzyme cascade systems can be very productive for the production of bioactive naringenin glucosides and quercetin rhamnoside products, using an easy and cheap system of regenerating NDPs sugars from sucrose. The modified products could have high pharmaceutical and cosmetic values. Therefore, here we developed cost-effective, eco-friendly, and sustainable systems to make glycosylated products by continuously synthesizing sugar donors in the glycosylation reaction systems. The use of abundantly available cheap sucrose as the primary source of sugar donor in GT-mediated reaction systems developed industrially applicable reactions. Sucrose synthase, which catalyzes the reversible conversion of sucrose and NDP into fructose and NDP-α-D-glucose, has been used to create a regenerative system of NDP-α-D-glucose, which was further modified to generate NDP-β-L-rhamnose. Both the systems were coupled with GTs, such as YjiC and UGT89C1, to synthesize target products. These results showed the feasibility of the use of sucrose as the source of various glyco-diversified natural products, using a cost-effective and sustainable approach.

Compliance with ethical standards This article does not contain any studies with human participants or animals performed by any of the authors.

Conflict of interest The authors declare that they have no conflict of interest.

References

Antonopoulou I, Varriale S, Topakas E, Rova U, Christakopoulos P, Faraco V (2016) Enzymatic synthesis of bioactive compounds with high potential for cosmeceutical application. Appl Microbiol Biotechnol 100:6519–6543

Bradford MM (1976) A rapid and sensitive method for the quantitation of microgram quantities of protein utilizing the principle of protein-dye binding. Anal Biochem 72:248–254

Cavia-Saiz M, Busto MD, Pilar-Izquierdo MC, Ortega N, Perez-Mateos M, Muñiz P (2010) Antioxidant properties, radical scavenging activity, and biomolecule protection capacity of flavonoid naringenin and its glycoside naringin: a comparative study. J Sci Food Agric 90: 1238–1244

Chouhan S, Sharma K, Zha J, Guleria S, Koffas MA (2017) Recent advances in the recombinant biosynthesis of polyphenols. Front Microbiol 8:2259

Danishefsky SJ, Bilodeau MT (1996) Glycals in organic synthesis: the evolution of comprehensive strategies for the assembly of oligosaccharides and glycoconjugates of biological consequence. Angew Chem Int Ed 35:1380–1419

Darsandhari S, Pandey RP, Shrestha B, Parajuli P, Liou K, Sohng JK (2018) One-pot multienzyme cofactors recycling (OPME-CR) system for lactose and non-natural saccharide conjugated polyphenol production. J Agric Food Chem 66:7965–7974

Daudé D, André I, Monsan P, Remaud-Siméon M (2014) Successes in engineering glucansucrases to enhance glycodiversification. In: Rauter AP, Lindhorst T, Queneau Y (eds) Carbohydrate Chemistry, Volume 40. The Royal Society of Chemistry, Cambridge, pp 624–645

De Bruyn F, Maertens J, Beauprez J, Soetaert W, De Mey M (2015) Biotechnological advances in UDP-sugar based glycosylation of small molecules. Biotechnol Adv 33:288–302

Deng X, Wang Z, Liu J, Xiong S, Xiong R, Cao X, Tang G (2017) Design, synthesis and biological evaluation of flavonoid salicylate derivatives as potential anti-tumor agents. RSC Adv 7:38171–38178

Diricks M, Gutmann A, Debacker S, Dewitte G, Nidetzky B, Desmet T (2017) Sequence determinants of nucleotide binding in sucrose synthase: improving the affinity of a bacterial sucrose synthase for UDP by introducing plant residues. Protein Eng Des Sel 30:143–150

Du G, Jin L, Han X, Song Z, Zhang H, Liang W (2009) Naringenin: a potential immunomodulator for inhibiting lung fibrosis and metastasis. J Cancer Res Ther 69:3205–3212

Felgines C, Texier O, Morand C, Manach C, Scalbert A, Régerat F, Rémésy C (2000) Bioavailability of the flavanone naringenin and its glycosides in rats. Am J Physiol Gastrointest Liver Physiol 279: G1148–G1154

Figueroa CM, Asención Diez MD, Kuhn ML, McEwen S, Salerno GL, Iglesias AA, Ballicora MA (2013) The unique nucleotide specificity of the sucrose synthase from *Thermosynechococcus elongatus*. FEBS Lett 587:165–169

Gantt RW, Peltier-Pain P, Thorson JS (2011) Enzymatic methods for glyco (diversification/randomization) of drugs and small molecules. Nat Prod Rep 28:1811–1853

Gurung RB, Kim EH, Oh TJ, Sohng JK (2013) Enzymatic synthesis of apigenin glucosides by glucosyltransferase (YjiC) from Bacillus licheniformis. DSM Mol Cell 36:355–361

Gutmann A, Bungaruang L, Weber H, Leypold M, Breinbauer R, Nidetzky B (2014) Towards the synthesis of glycosylated dihydrochalcone natural products using glycosyltransferase-catalysed cascade reactions. Green Chem 16:4417–4425

Gutmann A, Lepak A, Diricks M, Desmet T, Nidetzky B (2017) Glycosyltransferase cascades for natural product glycosylation: use of plant instead of bacterial sucrose synthases improves the UDP-glucose recycling from sucrose and UDP. Biotechnol J 12:1600557

He X, Ou HY, Yu Q, Zhou X, Wu J, Liang J (2015) Analysis of a genomic island housing genes for DNA S-modification system in *Streptomyces lividans 66* and its counterparts in other distantly related bacteria. Mol Microbiol 65:1034–1048

Jang SW, Cho CH, Jung YS, Rha C, Nam TG, Kim DO, Baek NI, Park CS, Lee BH, Shin HS, Seo DH, Lee SY (2018) Enzymatic synthesis of α-flavone glucoside via regioselective transglucosylation by amylosucrase from *Deinococcus geothermalis*. PLoS One 13: e0207466

Khan AW, Kotta S, Ansari SH, Sharma RK, Ali J (2015) Enhanced dissolution and bioavailability of grapefruit flavonoid naringenin by solid dispersion utilizing fourth generation carrier. Drug Dev Ind Pharm 41:772–779

Kim HJ, Kim BG, Ahn JH (2013) Regioselective synthesis of flavonoid bisglycosides using *Escherichia coli* harboring two glycosyltransferases. Appl Microbiol Biotechnol 97:5275–5282

Kim B, Park H, Na D, Lee SY (2014) Metabolic engineering of *Escherichia coli* for the production of phenol from glucose. Biotechnol J 9:621–629

Kim BG, Yang SM, Kim SY, Cha MN, Ahn JH (2015) Biosynthesis and production of glycosylated flavonoids in *Escherichia coli*: current state and perspectives. Appl Microbiol Biotechnol 99:2979–2988

Koirala N, Pandey RP, Parajuli P, Jung HJ, Sohng JK (2014) Methylation and subsequent glycosylation of 7, 8-dihydroxyflavone. J Biotechnol 184:128–137

Kumar S, Pandey AK (2013) Chemistry and biological activities of flavonoids: an overview. Sci World J 2013:162750

Le TT, Pandey RP, Gurung RB, Dhakal D, Sohng JK (2014) Efficient enzymatic systems for synthesis of novel α-mangostin glycosides exhibiting antibacterial activity against gram-positive bacteria. Appl Microbiol Biotechnol 98:8527–8538

Lee BH, Pyo MK, Lee JH, Choi SH, Shin TJ, Lee SM, Yun-Choi HS (2008) Differential regulations of quercetin and its glycosides on ligand-gated ion channels. Biol Pharm Bull 31:611–617

Lee HS, Kim TS, Parajuli P, Pandey RP, Sohng JK (2018) Sustainable production of dihydroxybenzene glucosides using immobilized amylosucrase from Deinococcus geothermalis. J Microbiol Biotechnol 28:1447–1456

Leonardi T, Vanamala J, Taddeo SS, Davidson LA, Murphy ME, Patil BS, Turner ND (2010) Apigenin and naringenin suppress colon carcinogenesis through the aberrant crypt stage in azoxymethane-treated rats. Exp Biol Med 235:710–717

Lewandowska U, Szewczyk K, Hrabec E, Janecka A, Gorlach S (2013) Overview of metabolism and bioavailability enhancement of polyphenols. J Agric Food Chem 61:12183–12199

Manach C, Donovan JL (2004) Pharmacokinetics and metabolism of dietary flavonoids in humans. Free Radic Res 38:771–785

Masada S, Kawase Y, Nagatoshi M, Oguchi Y, Terasaka K, Mizukami H (2007) An efficient chemoenzymatic production of small molecule glucosides with in situ UDP-glucose recycling. FEBS Lett 581:2562–2566

Mei YZ, Liu RX, WangDP WX, Dai CC (2015) Biocatalysis and biotransformation of resveratrol in microorganisms. Biotechnol Lett 37:9–18

Muthana MM, Qu J, Li Y, Zhang L, Yu H, Ding L, Chen X (2012) Efficient one-pot multienzyme synthesis of UDP-sugars using a promiscuous UDP-sugar pyrophosphorylase from Bifidobacterium longum (BLUSP). Chem Commun 48:2728–2730

Myung SK, Kim Y, Ju W, Choi HJ, Bae WK (2009) Effects of antioxidant supplements on cancer prevention: meta-analysis of randomized controlled trials. Ann Oncol 21:166–179

Nicolaou KC, Mitchell HJ (2001) Adventures in carbohydrate chemistry: new synthetic technologies, chemical synthesis, molecular design, and chemical biology. Angew Chem Int Ed 40:1576–1624

Panche AN, Diwan AD, Chandra SR (2016) Flavonoids: an overview. J Nutr Sci 5:e47

Pandey RP, Li TF, Kim EH, Yamaguchi T, Park YI, Kim JS, Sohng JK (2013) Enzymatic synthesis of novel phloretin glucosides. Appl Environ Microbiol 79:3516–3521

Pandey RP, Parajuli P, Shin JY, Lee J, Lee S, Hong YS, Sohng JK (2014) Enzymatic biosynthesis of novel resveratrol glucoside and glycoside derivatives. Appl Environ Microbiol 80:7235–7243

Pandey RP, Parajuli P, Chu LL, Darsandhari S, Sohng JK (2015) Biosynthesis of amino deoxy-sugar-conjugated flavonol glycosides by engineered Escherichia coli. Biochem Eng J 101:191–199

Pandey RP, Parajuli P, Koffas MAG, Sohng JK (2016) Microbial production of natural and non-natural flavonoids: pathway engineering, directed evolution and systems/synthetic biology. Biotechnol Adv 34:634–662

Parajuli P, Pandey RP, Trang NTH, Oh TJ, Sohng JK (2015) Expanded acceptor substrates flexibility study of flavonol 7-O-rhamnosyltransferase, AtUGT89C1 from Arabidopsis thaliana. Carbohydr Res 418:13–19

Park H, Kim J, Park JH, Baek NI, Park CS, Lee HS, Cha J (2012) Bioconversion of piceid to piceid glucoside using amylosucrase from Alteromonas macleodii deep ecotype. J Microbiol Biotechnol 22:1698–1704

Pei J, Chen A, Zhao L, Cao F, Ding G, Xiao W (2017) One-pot synthesis of hyperoside by a three-enzyme cascade using a UDP-galactose regeneration system. J Agric Food Chem 65:6042–6048

Qin L, Jin L, Lu L, Lu X, Zhang C, Zhang F, Liang W (2011) Naringenin reduces lung metastasis in a breast cancer resection model. Protein Cell 2:507–516

Roepke J, Bozzo GG (2013) Biocatalytic synthesis of quercetin 3-O-glucoside-7-O-rhamnoside by metabolic engineering of Escherichia coli. ChemBioChem 14:2418–2422

Rosencrantz RR, Lange B, Elling L (2014) Chemo-enzymatic cascade reactions for the synthesis of glycoconjugates. In: Riva S, Fessner WD (eds) Cascade biocatalysis. Wiley, Weinheim, pp 133–160

Rouseff RL, Martin SF, Youtsey CO (1987) Quantitative survey of narirutin, naringin, hesperidin, and neohesperidin in citrus. J Agric Food Chem 35:1027–1030

Schmölzer K, Gutmann A, Diricks M, Desmet T, Nidetzky B (2016) Sucrose synthase: a unique glycosyltransferase for biocatalytic glycosylation process development. Biotechnol Adv 34:88–111

Schmölzer K, Lemmerer M, Gutmann A, Nidetzky B (2017) Integrated process design for biocatalytic synthesis by a leloir glycosyltransferase: UDP-glucose production with sucrose synthase. Biotechnol Bioeng 114:924–928

Shiloach J, Fass R (2005) Growing E. coli to high cell density – a historical perspective on method development. Biotechnol Adv 23:345–357

Shomar H, Gontier S, van den Broek NJ, Mora HT, Noga MJ, Hagedoorn PL, Bokinsky G (2018) Metabolic engineering of a carbapenem antibiotic synthesis pathway in Escherichia coli. Nat Chem Biol 1:794–800

Simkhada D, Kurumbang NP, Lee HC, Sohng JK (2010) Exploration of glycosylated flavonoids from metabolically engineered E. coli. Biotechnol Bioprocess Eng 15:754–760

Teles Y, Souza M (2018) Sulphated flavonoids: biosynthesis, structures, and biological activities. Molecules 23:480

Terasaka K, Mizutani Y, Nagatsu A, Mizukami H (2012) In situ UDP-glucose regeneration unravels diverse functions of plant secondary product glycosyltransferases. FEBS Lett 586:4344–4350

Tian Y, Xu W, Zhang W, Zhang T, Guang C, Mu W (2018) Amylosucrase as a transglucosylation tool: from molecular features to bioengineering applications. Biotechnol Adv 36:1540–1552

Trantas EA, Koffas MA, Xu P, Ververidis F (2015) When plants produce not enough or at all: metabolic engineering of flavonoids in microbial hosts. Front Plant Sci 6:7

Xiao J, Muzashvili TS, Georgiev MI (2014) Advances in the biotechnological glycosylation of valuable flavonoids. Biotechnol Adv 32:1145–1156

Xie L, Zhang L, Wang C, Wang X, Xu YM, YuH WX (2018) Methylglucosylation of aromatic amino and phenolic moieties of drug-like biosynthons by combinatorial biosynthesis. Proc Natl Acad Sci 115:E4980–E4989

Xu L, Qi T, Xu L, Lu L, Xiao M (2016) Recent progress in the enzymatic glycosylation of phenolic compounds. J Carbohydr Chem 35:1–23

Yıldız SZ, Küçükislamoğlu M, Tuna M (2009) Synthesis and characterization of novel flavonoid-substituted phthalocyanines using (±) naringenin. J Org Chem 694:4152–4161

Yin R, Han K, Heller W, Albert A, Dobrev PI, Zažímalová E, Schäffner AR (2014) Kaempferol 3-*O*-rhamnoside-7-*O*-rhamnoside is an endogenous flavonol inhibitor of polar auxin transport in *Arabidopsis* shoots. New Phytol 201:466–475

Yuan S, Yin S, Liu M, Kong JQ (2018) Isolation and characterization of a multifunctional flavonoid glycosyltransferase from *Ornithogalum caudatum* with glycosidase activity. Sci Rep 8:5886

Zhang YX, Chen SL (2006) Molecular identification, polymorphism, and expression analysis of major histocompatibility complex class IIA and B genes of turbot (*Scophthalmus maximus*). Mar Biotechnol 8: 611–623

Zhang J, Singh S, Hughes RR, Zhou M, Sunkara M, Morris AJ, Thorson JS (2014) A simple strategy for glycosyltransferase-catalyzed aminosugar nucleotide synthesis. ChemBioChem 15:647–651

Publisher's note Springer Nature remains neutral with regard to jurisdictional claims in published maps and institutional affiliations.